Journal of Environmental Science and Management 23-1: 39-49 (June 2020) ISSN 0119-1144

Exploring Spatial Relationship Between Electrical Conductivity and Spectral Salinity Indices in the Mekong Delta

ABSTRACT

The negative impact of salinization concurrent with drought is a severe problem that creates challenges for agriculture in deltas and coastal lowlands. This study aims to investigate the spatial relationship among the field measured electrical conductivity (EC) and spectral salinity indices derived from Remote sensed data in the Mekong Delta using Geographically Weighted Regression (GWR). A wide range of Landsat 8 Operational Land Images (OLI) products, including single bands, band ratios, vegetation indices (NDVI and EVI), intensity indices (INT), and brightness indices (BI) were employed for computing salinity indices. The Kriging and Co-kriging interpolation techniques were used to estimate the spatial pattern of the field measured EC. Additionally, the Ordinary Least Square (OLS) regression were employed to characterize the relationship between single bands and EC measurement before applying the GWR for exploring the spatial correlation among the indices. There was a gradually increased of EC value from inland to coastal area. A significant relationship between EC measurement and spectral salinity indices and the highest correlation coefficient with p value less than 0.05 was found in EVI (r^2 = 0.736). This study demonstrated that the GWR is germane to analyse the spatial correlation among the mentioned variables in the study area. Moreover, it also revealed that spectral salinity indices could be an alternative option for EC measurement in monitoring salt water intrusion at coastal areas.

Thuong V. Tran[1,2*]
Duy X. Tran[3]
Hoa V. Pham[4,5]
Tuan V. Truong[2]
Hoanh P. Trinh[6]
Dung Q. Nguyen[4]
Binh A. Nguyen[4]
Hanh C. Nguyen[4]

[1] School of Geography, University of Social Sciences and Humanities, VNU-HCM, HCMC, 70000, Vietnam
[2] School of Geography, Ho Chi Minh City University of Education, HCMC, 70000, Vietnam
[3] School of Agriculture and Environment, Massey University, Palmerston North 4442, New Zealand
[4] Ho Chi Minh City Institute of Resources Geography, Vietnamese Academy of Science and Technology, HCMC 70000, Vietnam
[5] Graduate University of Science and Technology, Vietnamese Academy of Science and Technology, Hanoi 10000, Viet Nam
[6] School of Education for Social Sciences, Saigon University, HCMC 70000, Vietnam;

*corresponding author: tvthuong@hcmussh.edu.vn

Key words: *Geographically Weighted Regression, Salinization, Salinity Index, EC measurement, Ben Tre*

INTRODUCTION

Soil salinization is a common problem in deltas and coastal lowlands where are characterized by high groundwater tables, insufficient drainage networks, and seawater intrusion (*Scudiero et al. 2016*). It exerts negative effects on plant growth, agricultural productivity, soil, and water quality as well as increases soil erosion, especially in semi-arid and arid regions (*Allbed et al.2014*). In fact, electrical conductivity (EC) has been widely used to determine salinity content (*Dellavalle 1992; Douaik et al. 2004; Rahman 2016; Sonmez et al. 2008*) but this traditional method is expensive (*Ibrahim 2016*) and is limited capability in reflecting spatial trend of salinization (*Wu et al. 2008*). It is necessary to use higher resolution data to characterize salinity trend and pattern. Detailed mapping of salinization will enable to evaluate the effectiveness of controlling practices for salt-content.

In recent decades, several studies have been carried out based on the potential of remote sensing using multispectral (*Paliwal et al. 2018; Rahmati and*

Hamzehpour 2017; Tran et al. 2019) and microwave data (*Baghdadi et al. 2007; Barbouchi et al. 2015; Hoa et al. 2019*) as providing quickly, timely, relatively cheap, and repetitive data. Various types of spectral salinity indices have been applied to characterize the salinity pattern under the groups of single bands, band ratios, vegetation indices, intensity indices, and brightness indices. However, the effectiveness of the remote sensed salinity index is depended on several factors such as natural conditions, system features, agricultural practices, and drainage management in particular geographic region (*Wu et al. 2008*). Hence, it is suggested to find appropriate spectral salinity index for particular area.

In fact, many studies have successfully applied the Pearson correlation and the Ordinary Least Square (OLS) regression (*Rahmati and Hamzehpour 2017; Shammi et al. 2017*) to examine the relationship between the EC and spectral salinity indices for selecting the most appropriate spectral salinity index. Results from these models reveal a general trend for whole study area while this implication varies across space (*Goovaerts et al. 2015; Ivajnšič et al. 2014*). Compared to other spatial multivariate regression, Geographically Weighted Regression (GWR) has been investigated as an efficient method for solving non-stationarity through generating several kernels (*Mondal et al. 2015; Szymanowski and Kryza 2011*). This model is able to use to obtain the correlation among EC measurement and spectral salinity indices derived from satellite imagery at the pixel level. In our study, we aimed to discover the local relationship between the EC measurement of collected soil samples and spectral salinity indices so the GWR was utilized instead of using Pearson and OLS in the study area.

Overall, the main goals of this study were to examine the spatial distribution of the fields measured EC; demonstrate the effectiveness of GWR in determining spatial correlation among EC measurement and spectral salinity indices; and select the most effective spectral index for estimate salinity situation in agricultural land. Ben Tre province was selected to implement the research because it is affected severely by salinization (*Nguyen 2017; Tran et al. 2019*). Results from this study provided an alternative option to EC measurement in mapping salinity in the Mekong Delta.

MATERIAL AND METHODS

Study site description

Ben Tre is one of the coastal provinces in Vietnam, extended between 9048'N-10020'N and 106048'E-105057'E. The province is located in the Mekong River Delta (MRD) and covers an area of 2,360 km^2. It borders with East Sea and has four main estuaries: Dai, Ba Lai, Ham Luong, and Co Chien (**Figure 1**). Hence, it is easily implicated by the mixing of river and

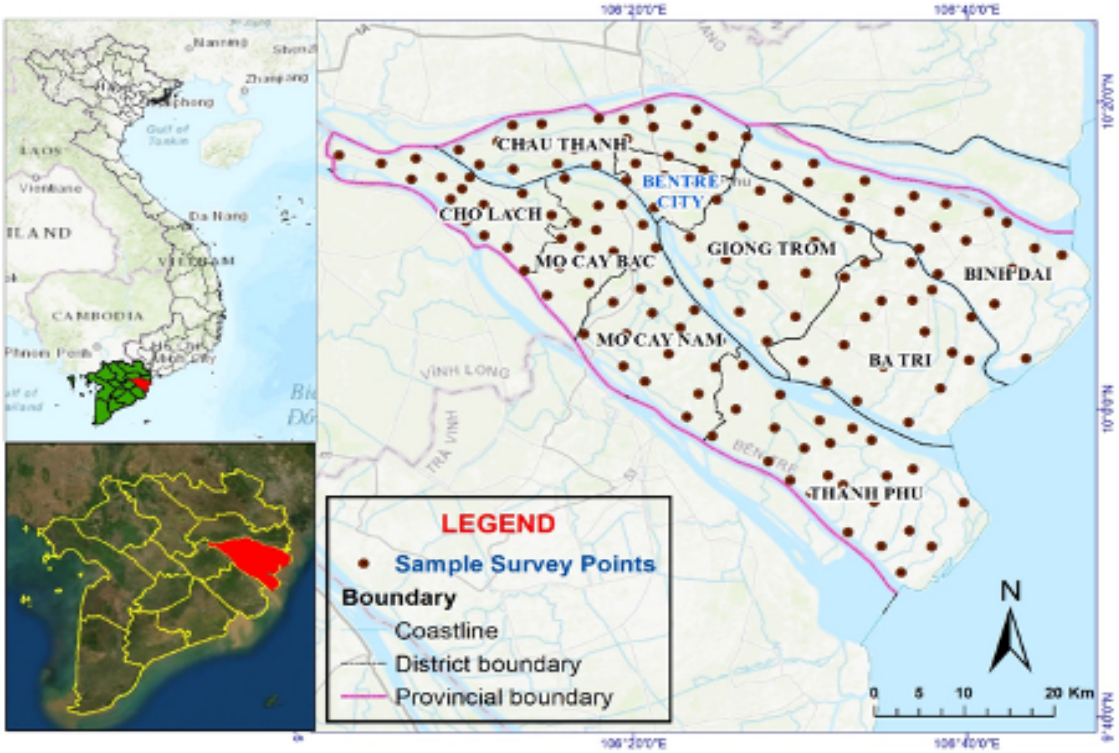

Figure 1. Location and sample survey points in the study site.

ocean dynamic around year and the influence of salt water intrusion concurrent with drought through these river mouths (*My and Vuong 2006*). Besides, it has flat terrain and multi-channel estuaries consisting of many damped branches due to a relatively strong river discharge, even during the dry season (*Nguyen et al. 2008; Sâm 2003*). Salinization, therefore, may exacerbate under the combined effect of sea level rise and reduction of flow upstream in the dry season in the MRD (*Hoa et al. 2019; Vu et al. 2018*).

Soil Sampling

The field observation of the electrical conductivity (EC) was collected in April 2018 (n = 150) within the study area (**Figure 1**). Soil samples at a 0-100 cm depth were taken and analysed for their EC in paste situation extracts (Laboratory of Soil Recourses Department, Ho Chi Minh City Institute of Recourses Geography). Electrical conductivity (EC) was determined in soil liquid solution using conductivity meter with the soil and water dilution at ratio of 1:5 (*Lesch et al. 1992; Sharma et al. 2017*). The EC classification was ranged to examine salinity situation (**Table 1**).

Table 1. Categories of EC.

Dynamic range	Description	EC (*mS/cm*)
S0	None Salinity	2 or less
S1	Near Salinity	2 to 4
S2	Moderate Salinity	4 to 8
S3	Extreme Salinity	above 8

Spectral Indices

The parameters for calculating spectral indices derived from Landsat 8OLI data around April 2018 were obtained from Google Earth Engine. A wide range of Landsat OLI products, including Vegetation Indices (NDVI and EVI), Water Index (NDWI), Blue Band, Green Band, Red Band, Near Infrared Band, Short-Wave Infrared Band (SWIR) were main resources for computing salinity indices. Landsat data used in the study can be classified into five groups: original bands (Blue, Green, Red, Near Infrared, and Short-Wave Infrared Band), band ratios, salinity indices, intensity indices, brightness indices, and vegetation indices. These remotely sensed data were then correlated with grounds measured EC to determine the most appropriate index (**Table 2**).

Table 2. Summary of some widely used spectral indices for salinity assessment.

Formula	Numerical order	Formula	Numerical order
$R_1 = \frac{B}{G}$	(1)	$BI_2 = \sqrt{R^2 + NIR^2}$	(13)
$R_2 = \frac{B}{R}$	(2)	$NDVI = \frac{NIR - R}{NIR + R}$	(14)
$R_3 = \frac{B}{NIR}$	(3)	$EVI = \frac{2.5 \times (NIR - R)}{NIR + 6 \times R - 7.5 \times B + 1}$	(15)
$R_4 = \frac{G}{R}$	(4)	$SI_1 = \sqrt{R_B \times R_R}$	(16)
$R_5 = \frac{G}{NIR}$	(5)	$SI_2 = \sqrt{R_G \times R_R}$	(17)
$R_6 = \frac{R}{NIR}$	(6)	$SI_3 = \sqrt{R \times NIR}$	(18)
$R_7 = \frac{B \times R}{G}$	(7)	$SI_4 = \sqrt{G^2 + R^2}$	(19)
$R_8 = \frac{G \times R}{B}$	(8)	$SI_5 = \sqrt{R_G^2 + R_R^2 + R_{NIR}^2}$	(20)
$R_9 = \frac{R \times NIR}{G}$	(9)	$SI_6 = \frac{R - NIR}{R + NIR}$	(21)
$INT_1 = \frac{R + G}{2}$	(10)	$SI_7 = \sqrt{\frac{(\mathrm{NIR} \times \mathrm{R}) - (\mathrm{G} \times \mathrm{B})}{(\mathrm{NIR} \times \mathrm{R}) + (\mathrm{G} \times \mathrm{B})}}$	(22)
$INT_2 = \frac{G + R + NIR}{2}$	(11)	$SI_8 = \frac{SWIR_1}{SWIR_2}$	(23)
$BI_1 = \sqrt{G^2 + NIR^2}$	(12)	$SI_9 = \frac{SWIR_1 - SWIR_2}{SWIR_1 + SWIR_2}$	(24)

At the equations from (1)-(24), R_1 to R_9 are band ratios, which are better for identifying salts in soils and salt-stressed crops than individual bands (*Allbed et al. 2018; Iqbal and Mastorakis 2015; Masoud 2014*); INT_1 and INT_2 are the intensity indices of visible bands and near infrared spectral, respectively (*Douaoui et al. 2006; Rahmati and Hamzehpour 2017*); BI_1 and BI_2 are the brightness index (A*llbed et al. 2018; Khan et al. 2001*); NDVI is the normalized difference vegetation index (*Rahmati and Hamzehpour 2017; Taghadosi and Hasanlou 2017*); EVI is the enhanced vegetation index (*Huete et al. 2002; Lobell et al. 2010; Paliwal et al. 2018*); and SI1 to SI9 are types of salinity indices (*Asfaw et al. 2016; Masoud 2014; Rahmati and Hamzehpour 2017*).

Kriging and Co-kriging

Kriging and Co-kriging were used for interpolated the spatial distribution of the field measured EC via ArcGIS 10.7 software. The Kriging is a local determination method that uses the spatial dependence of a particular variable for the estimation procedure. It is as a perfect tool for estimating on the basis of a 10 m x 10 m grid (*Heisel et al. 1999*). Co-kriging is an extension of kriging to assess spatial correlation between two or more variables. This model reduces the complexity of the model by building independent Kriging (*Xiao et al. 2018*). The estimated value of the primary variable at location x_0 is:

$$\hat{z}_1(x_0) = \sum_{i=1}^{N_1} \lambda_{1i} z_1(x_{1i}) + \sum_{i=1}^{N_2} \lambda_{2j} z_2(x_{2j}) \quad (25)$$

where N_1 and N_2 are the number of neighbors of z_1 and z_2; λ_{1i} and λ_{2j} are the weights associated to each sampling point. When variables z_1=z_2 the system converts to kriging. The attribute is usually called the primary variable, especially geo-statistics.

Geographically Weighted Regression

GWR is a type of regression model, was developed by *Brunsdon et al.* (*1996*). It is a nonparametric model of spatial drift that relies on a sequence of locally linear regressions to produce estimates for every point in space by using a subset of information from nearby observations (*Szymanowski and Kryza 2012*). It is a relatively simple technique that extends the traditional regression framework of equation:

$$y_i = a_0 + \sum_{k=1,m} a_k x_{ik} + \varepsilon_i \quad (26)$$

where, y_i is the *i*-th observation of the dependent variable, x_{ik} is the *i*-th observation of the *k*-th independent variable, the ε_i are independent normally distributed error terms with zero means, and each ak must be determined from a sample of n observations. The method can be used to spatialize discrete point data on the assumption that auxiliary, independent variables are known and continuous in space, or, technically, they can be provided as raster layers.

RESULTS AND DISCUSSION

The spatial distribution of EC measurement and its relation to spectral reflectance bands

The measured EC distribution (**Figure 2**) and its correlation with single bands was derived from Landsat (**Figure 3**). Overall, the EC value decreased from coastal area to inland and it had a significant relationship with spectral reflectance bands.

The moderate and extreme salinity levels covered substantial areas of Thanh Phu, Ba Tri, and Binh Dai districts due to shrimp farming practices. The suitable shrimp culture is that saline content or EC value is over 4 (4*mS/cm*). Hence, it creates a salinity zone around the shrimp farming.

Besides, there were positive correlations (**Figure 3**) among EC measurement and Blue, Green, and Red bands with r value greater than zero, whereas the negative relationship with the highest correlation coefficients (r = -0.46) was found in the regression equation of the measured EC and NIR band. The single bands are primary input factors to compute saline spectral indices, ratio bands, and rest of indices in this study (**Table 2**). Therefore, conducting the relationship between EC measurement and single bands is important to discover the major input band. This is crucial to develop salinity index formulas and to test hypothesis from selecting the most effective index. It was explored that the NIR band reflected the most significant statistic, compared to the rest of bands in model.

The spatial relationship between EC and spectral indices

In general, a strong correlation among them was found, showing by the r^2 values from 0.597 to 0.736 (**Table 3**).

The highest correlation coefficients (r^2 = 0.7361) was found in the relationship between measured EC and EVI value that employed by the NIR, Red, and Blue bands, followed by the Eq. (15). It is valid that the EC

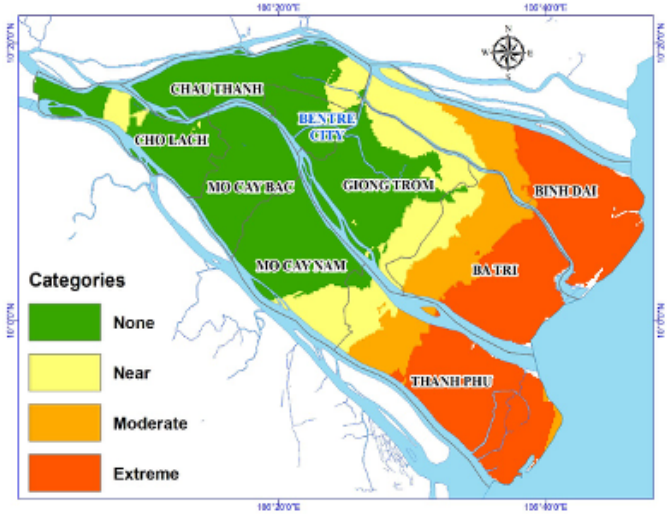

Figure 2. Descriptive statistics of EC and density using Kriging.

measurement and NIR band owned the highest *r* value (**Figure 3**). This value is consistent with the conclusions using machine learning algorithms and the Ordinary Least Square (OLS) drawn by *Hoa el al.* (*2019*) and *Tran et al.* (*2019*), respectively. In addition, several studies demonstrated that EVI has a high sensitivity to biomass, compared to other vegetation indices and it is more authentic to use while humidity is high (*Caccamo et al. 2011; Lobell et al. 2010; Paliwal et al. 2018*). Moreover, EVI is regarded as an optimum index since it is less sensitiveto soil and atmospheric variation and more responsive to canopy structure variations (*Lobell et al. 2010; Paliwal et al. 2018*).

The level of correlation varies across space and time (**Figure 4**) and the land use situation was provided by the Department of Natural Resources and Environment in the study area (**Figure 5**). The correlation maps showed both positive and negative relationship between the measured EC and spectral reflectance indices. This is different compared to what is commonly observed in the previous studies. Several authors explored that EC measurement are generally positively correlated with salinity indices (*Asfaw et al. 2016; Iqbal and Mastorakis 2015*). However, it is observed that the correlation among them may be different in specific circumstances. It can be proved that most of negative relationship focused in shrimp farming of coastal areas includes Thanh Phu, Binh Dai, and Ba Tri districts, while the positive correlation was explored in cropland areas (**Figure 5**). Several studies revealed that the EC change is significantly correlated with the land use change, whereas the salinity levels are controlled by saline concentration in soil, surface water or ground water (*Scudiero et al. 2015; Zheng et al. 2009*).

Previous studies conducted in the study area applied the Ordinary Least Square (OLS) for examining the correlation among EC measurement and spectral indices and then selecting the best spectral index, shown the highest r value, for determining the spatiotemporal pattern salinity variations (*Hoa et al. 2019; Tran et al. 2019*). However, the spatial distribution of salinity content is varied through geographical locations and various conditions (*Goovaerts et al. 2015; Ivajnšič et al. 2014*). Therefore, the relationship among remotely sensed data

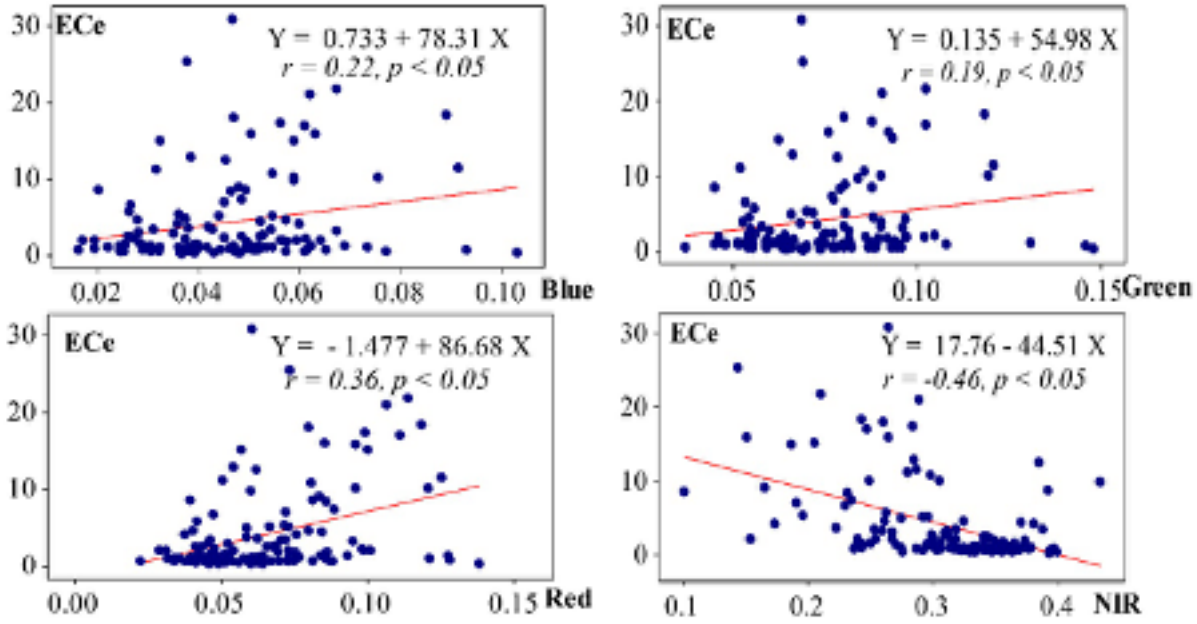

Figure 3. The OLS regression between ECe and single bands. All of models are statistically significant with $p<0.05$.

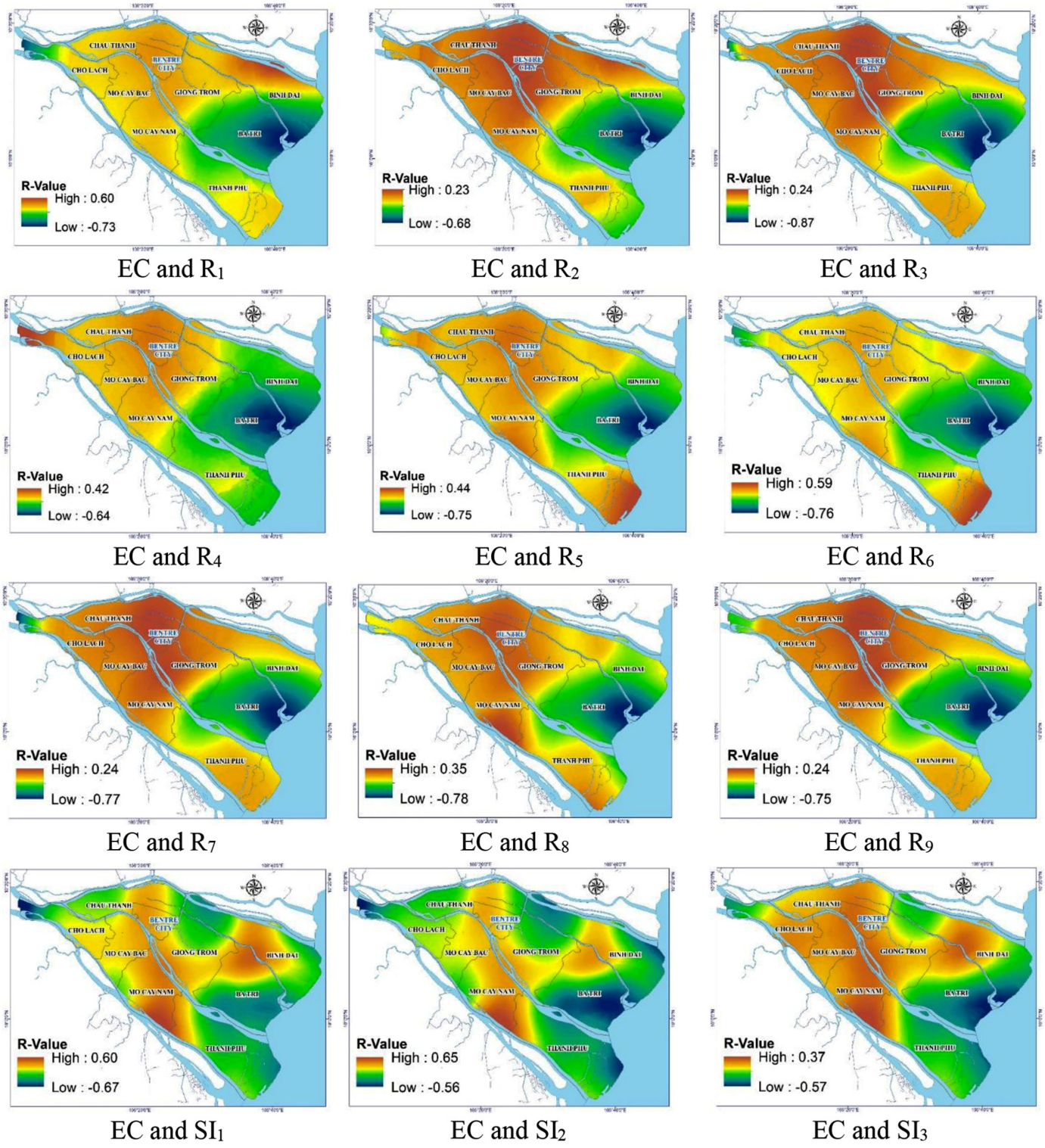

Figure 4. The spatiotemporal correlation between the measured EC and spectral indices.

and measured EC will be more accurate if it considers the spatial variations. The distribution of the measured EC using the Kriging and Co-Kriging provides an indication of salinity content from inland to coastal area in the province. In the next step, the correlation among single bands and EC measurement considered a significant statistic, cluster among input data, and validation of applying the GWR. Results from this study revealed that the GWR is an efficient method in examining spatial relationship among EC measurement

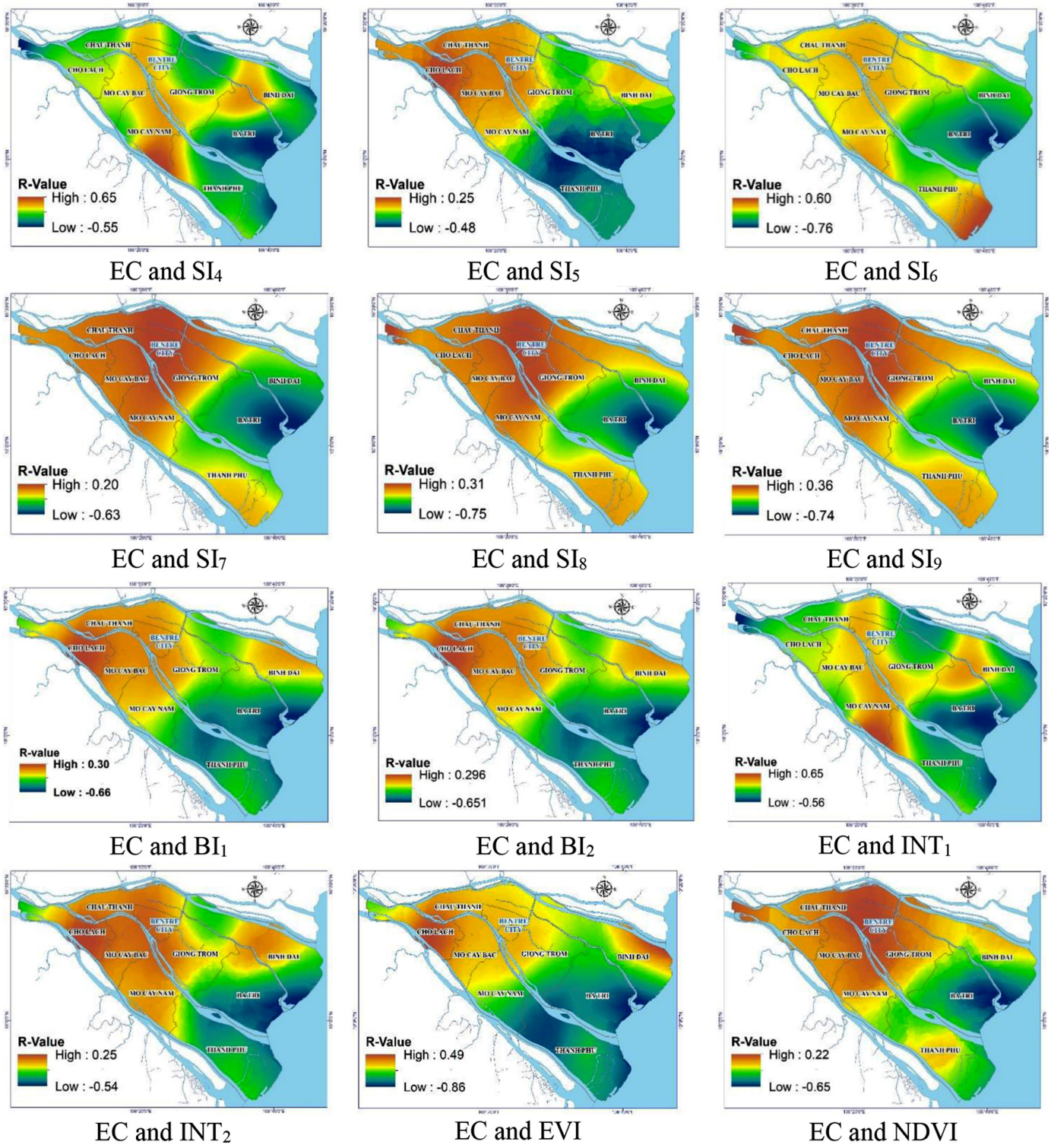

Figure 4. The spatiotemporal correlation between the measured EC and spectral indices (cont.).

and spectral indices, well-known as spatially independent and dependent variables, respectively. In the study area, each land use type reflects a different salinity level and the highest concentration of salinity mainly occurs in the dry season (from November to April). The various correlation among the variables through space in our research therefore, is reliable because it was conducted in separate land use and in the dry season.

Table 3. Summary of results from the GWR analysis between EC and ratio bands (R), salinity indices (SI), brightness (BI), intensity (INT), and vegetation indices (EVI and NDVI).

VARNAME	Band width	Residual Squares	Effective Number	Sigma	AICc	r^2
EC vs. R_1	6426.6	38.677	40.989	0.5957	300.18	0.7336
EC vs. R_2	7187	45.477	33.686	0.6253	308.4	0.6867
EC vs. R_3	8032.6	51.141	27.302	0.6456	313.19	0.6477
EC vs. R_4	7187	45.826	32.542	0.6246	307.26	0.6843
EC vs. R_5	6426.6	40.25	41.122	0.608	307.18	0.7227
EC vs. R_6	6426.6	38.892	41.237	0.598	302.48	0.7321
EC vs. R_7	8032.6	51.137	27.231	0.6454	313.14	0.6477
EC vs. R_8	6426.6	39.428	41.154	0.6019	304.77	0.7284
EC vs. R_9	8032.6	51.194	26.917	0.6449	312.13	0.6473
EC vs. SI_1	7446.7	47.477	40.348	0.658	328.73	0.6729
EC vs. SI_2	7272.5	45.43	41.896	0.6483	325.85	0.687
EC vs. SI_3	7482.1	46.412	39.34	0.6476	323.26	0.6803
EC vs. SI_4	7212.6	44.995	42.359	0.6465	325.52	0.69
EC vs. SI_5	8056.4	50.558	33.117	0.6577	322.59	0.6517
EC vs. SI_6	6426.6	38.966	41.18	0.5984	302.57	0.7316
EC vs. SI_7	10734	58.485	17.539	0.6645	314.96	0.5971
EC vs. SI_8	8032.6	51.144	27.21	0.6454	313.02	0.6477
EC vs. SI_9	8032.6	51.142	27.232	0.6454	313.12	0.6477
EC vs. BI_1	8056.4	50.365	33.001	0.6561	321.73	0.6531
EC vs. BI_2	8056.4	50.401	33.021	0.6564	321.88	0.6528
EC vs. INT_1	7255.4	45.296	42.013	0.6477	325.69	0.688
EC vs. INT_2	7734.1	48.591	36.029	0.653	323.03	0.6653
EC vs. NDVI	6426.6	38.965	41.18	0.5984	302.57	0.7316
EC vs. EVI	7385.3	43.026	38.68	0.6217	310	0.7361

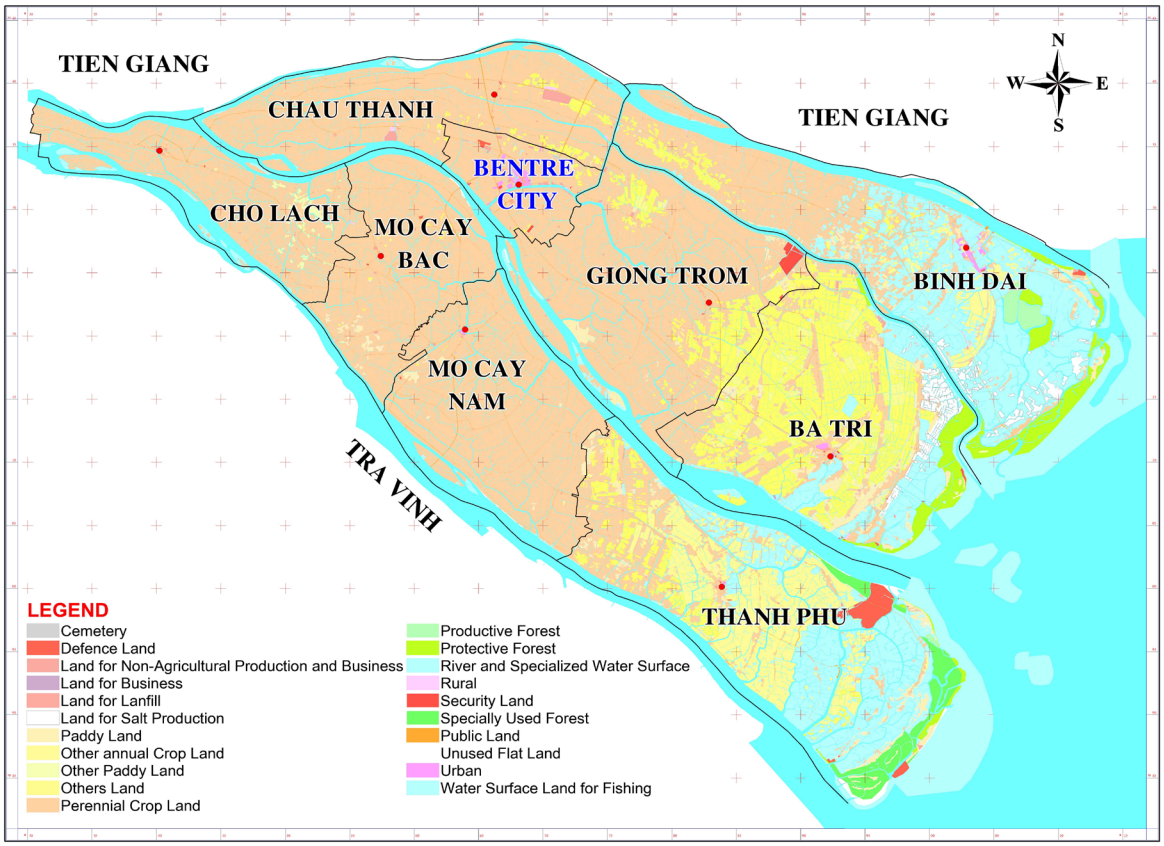

Figure 5. Land use in study area in 2018.

CONCLUSIONS AND RECOMMEDATIONS

This study performed regression analysis between soil EC values (measured at 150 random sampling points) and twenty-five spectral indices (derived from Landsat 8 OLI) in Ben Tre province, MRD. Both positive and negative relationships between EC and spectral indices were found in the study area. This gives a more detail and accurate picture of salinity distribution and therefore can be used as scientific basis for land and environmental planning and management. It is also discovered that the highest correlation was explored between EC measurements and EVI with $r^2 = 0.736$. This suggested that EVI can be used as a potential spectral index to monitor salinity at the pixel level, compared to other indices in the study area.

The spatial relationship among EC measurement and these indices was mapped using GWR. It showed that the correlation coefficients varied through separate land use types due to different conditions, such as soil types, densities, and policy management in land use in particular area (*Wu et al. 2008*). The negative relationship among them was explored in shrimp farming areas in coastal districts. This research once again confirmed the GWR is an effective model for tackling spatial correlation and fits exceptionally well into the study area. In addition, the study highlighted the significant practice of the EVI as an effective factor for modelling salinity and promised the high potential of remote sensing applications in agriculture. Besides, future work on the mapping salinity variations should include additional factors involving saline concentration (e.g. Chlorine and Total Dissolved Solids). It is also recommend that future study needs to compare the performance between using GWR and other spatially correlated modelling methods, such as Moran's index, Spatial Lag Model, Spatial Error Model, and Geary's coefficient.

Furthermore, there are several recommendations based on the results such as the government should propose a strategy for preventing tidal, controlling freshwater under the application of geospatial technology and spatial approaches; reinforcing coastal dikes, adding embankments around rivers to control sea level rise entering domestic area; investing to modernize irrigation systems, automated monitoring systems, proactive operation, and updating continuously information about water quality on social network; and the local farmers should use water supply at canals suitably following the regulations of government in the dry season.

REFERENCES

Allbed, A., Kumar, L., and Sinha, P. 2014. "Mapping and modelling spatial variation in soil salinity in the Al Hassa Oasis based on remote sensing indicators and regression techniques" *Remote Sensing* 6: 1137–1157.

Allbed, A., Kumar, L., and Sinha, P. 2018. "Soil salinity and vegetation cover change detection from multi-temporal remotely sensed imagery in Al Hassa Oasis in Saudi Arabia" *Geocarto International* 33: 830–846.

Asfaw, E., Suryabhagavan, K. V., and Argaw, M. 2016. "Soil salinity modeling and mapping using remote sensing and GIS: the case of Wonji sugar cane irrigation farm, Ethiopia" *Journal of the Saudi Society of Agricultural Sciences* 17 (3):250-258.

Baghdadi, N., Aubert, M., Cerdan, O., Franchistéguy, L., Viel, C., Eric, M., Zribi, M., and Desprats, J. F. 2007. "Operational mapping of soil moisture using synthetic aperture radar data: application to the Touch basin (France)" *Sensors* 7: 2458–2483.

Barbouchi, M., Abdelfattah, R., Chokmani, K., Aissa, N. B., Lhissou, R., and El Harti, A. 2015. "Soil salinity characterization using polarimetric InSAR coherence: Case studies in Tunisia and Morocco" *IEEE Journal of Selected Topics in Applied Earth Observations and Remote Sensing* 8: 3823–3832.

Brunsdon, C., Fotheringham, A. S., and Charlton, M. E. 1996. "Geographically weighted regression: a method for exploring spatial non-stationarity" *Geographical analysis* 28: 281–298.

Caccamo, G., Chisholm, L. A., Bradstock, R. A., and Puotinen, M. L. 2011. "Assessing the sensitivity of MODIS to monitor drought in high biomass ecosystems" *Remote Sensing of Environment* 115: 2626–2639.

Dellavalle, N. B. 1992. "Handbook on reference methods for soil analysis," *Quality Assurance Plans for Agricultural Testing Laboratories* 1: 18–32.

Douaik, A., Van Meirvenne, M., Tóth, T., and Serre, M. 2004. "Space-time mapping of soil salinity using probabilistic Bayesian maximum entropy" *Stochastic Environmental Research and Risk Assessment* 18: 219–227.

Douaoui, A. E. K., Nicolas, H., and Walter, C. 2006. "Detecting salinity hazards within a semiarid context by means of combining soil and remote-sensing data" *Geoderma* 134: 217–230.

Goovaerts, P., Xiao, H., Adunlin, G., Ali, A., Tan, F., Gwede, C. K., and Huang, Y. 2015. "Geographically-weighted regression analysis of percentage of late-stage prostate

cancer diagnosis in Florida" *Applied Geography* 62: 191–200.

Heisel, T., Ersbøll, A. K., and Andreasen, C. 1999. "Weed mapping with co-kriging using soil properties," *Precision Agriculture* 1: 39–52.

Hoa, P. V., Giang, N. V., Binh, N. A., Hai, L. V. H., Pham, T.-D., Hasanlou, M., and Tien Bui, D. 2019. "Soil Salinity Mapping Using SAR Sentinel-1 Data and Advanced Machine Learning Algorithms: A Case Study at Ben Tre Province of the Mekong River Delta (Vietnam)" *Remote Sensing* 11: 128.

Huete, A., Didan, K., Miura, T., Rodriguez, E. P., Gao, X., and Ferreira, L. G. 2002. "Overview of the radiometric and biophysical performance of the MODIS vegetation indices" *Remote Sensing of Environment* 83: 195–213.

Ibrahim, M. 2016. "Modeling Soil Salinity and Mapping Using Spectral Remote Sensing Data in the Arid and Semi-Arid Region" *International Journal of Remote Sensing Applications* 6: 76–83.

Iqbal, S., and Mastorakis, N. 2015. "Soil salinity detection using RS data," *Advances in Environmental Science and Energy Planning* 1: 277–81.

Ivajnšič, D., Kaligarič, M., and Žiberna, I. 2014. "Geographically weighted regression of the urban heat island of a small city" *Applied Geography* 53: 341–353.

Khan, N. M., Rastoskuev, V. V., Shalina, E. V., and Sato, Y. 2001. "Mapping salt-affected soils using remote sensing indicators-a simple approach with the use of GIS IDRISI". Paper presented at the 22nd Asian Conference on Remote Sensing. Singapore. November 2001. Lesch, S. M., Rhoades, J. D., Lund, L. J., and Corwin, D. L. 1992. "Mapping soil salinity using calibrated electromagnetic measurements" *Soil Science Society of America Journal* 56: 540–548.

Lobell, D. B., Lesch, S. M., Corwin, D. L., Ulmer, M. G., Anderson, K. A., Potts, D. J., Doolittle, J. A., Matos, M. R., and Baltes, M. J. 2010. "Regional-scale assessment of soil salinity in the Red River Valley using multi-year MODIS EVI and NDVI" J*ournal of Environmental Quality* 39: 35–41.

Masoud, A. A. 2014. "Predicting salt abundance in slightly saline soils from Landsat ETM+ imagery using spectral mixture analysis and soil spectrometry" *Geoderma* 217: 45–56.

Mondal, B., Das, D. N., and Dolui, G. 2015. "Modeling spatial variation of explanatory factors of urban expansion of Kolkata: a geographically weighted regression approach" *Modeling Earth Systems and Environment* 1: 29.

My, T., and Vuong, N. D. 2006. "Salinity Intrusion Trend in River and Canal Systems and Some Prevention Methods in Ben Tre Province". Paper presented at the Vietnam and Japan Estuary Workshop. Hoi An, Vietnam. September 2015.

Nguyen, A. D., Savenije, H. H., Pham, D. N., and Tang, D. T. 2008. "Using salt intrusion measurements to determine the freshwater discharge distribution over the branches of a multi-channel estuary: The Mekong Delta case" *Estuarine, Coastal and Shelf Science* 77: 433–445.

Nguyen, N. A. 2017. "Historic drought and salinity intrusion in the Mekong Delta in 2016: Lessons learned and response solutions" *Vietnam Journal of Science, Technology and Engineering* 59: 93–96.

Paliwal, A., Laborte, A., Nelson, A., and Singh, R. K. 2018. "Salinity stress detection in rice crops using time series MODIS VI data" *International Journal of Remote Sensing* 1:–17.

Rahman, M. T. 2016. "Detection of land use/land cover changes and urban sprawl in Al-Khobar, Saudi Arabia: An analysis of multi-temporal remote sensing data" ISPRS *International Journal of Geo-Information* 5: 15.

Rahmati, M., and Hamzehpour, N. 2017. "Quantitative remote sensing of soil electrical conductivity using ETM+ and ground measured data" *International Journal of Remote Sensing* 38: 123–140.

Sâm, L. 2003. Xâm nhập mặn ở đồng bằng Sông Cửu Long. NXB Nông nghiệp.

Scudiero, E., Skaggs, T. H., and Corwin, D. L. 2015. "Regional-scale soil salinity assessment using Landsat ETM+ canopy reflectance" *Remote Sensing of Environment* 169: 335–343.

Scudiero, E., Skaggs, T. H., and Corwin, D. L. 2016. "Comparative regional-scale soil salinity assessment with near-ground apparent electrical conductivity and remote sensing canopy reflectance" *Ecological Indicators* 70: 276–284.

Shammi, M., Rahman, M. M., Islam, M. A., Bodrud-Doza, M., Zahid, A., Akter, Y., Quaiyum, S., and Kurasaki, M. 2017. "Spatio-temporal assessment and trend analysis of surface water salinity in the coastal region of Bangladesh" *Environmental Science and Pollution Research* 24: 14273–14290.

Sharma, R., Bell, R.W., Wong, M.T.F., 2017. "Dissolved reactive phosphorus played a limited role in phosphorus transport via runoff, through flow and leaching on contrasting cropping soils from southwest Australia" *Science of the Total Environment* 577: 33–44. https://doi.org/10.1016/j.scitotenv.2016.09.182.

Sonmez, S., Buyuktas, D., Okturen, F., and Citak, S. 2008. "Assessment of different soil to water ratios (1: 1, 1: 2.5, 1: 5) in soil salinity studies" *Geoderma* 144: 361–369.

Szymanowski, M., and Kryza, M. 2011. "Application of geographically weighted regression for modelling the spatial structure of urban heat island in the city of Wroclaw (SW Poland)" *Procedia Environmental Sciences* 3: 87–92.

Szymanowski, M., and Kryza, M. 2012. "Local regression models for spatial interpolation of urban heat island—an example from Wrocław, SW Poland" *Theoretical and Applied Climatology* 108: 53–71.

Taghadosi, M. M., and Hasanlou, M. 2017. "Trend Analysis of Soil Salinity in Different Land Cover Types Using Landsat Time Series Data (Case Study Bakhtegan Salt Lake)". *International Archives of the Photogrammetry, Remote Sensing & Spatial Information Sciences* 42 (4): 251-257.

Tran, T. V., Tran, D. X., Myint, S. W., Huang, C., Pham, H. V., Luu, T. H., and Vo, T. M. T. 2019. "Examining spatiotemporal salinity dynamics in the Mekong River Delta using Landsat time series imagery and a spatial regression approach" *Science of The Total Environment* 687: 1087-1097.

Vu, N. N., Trung, L. V., and Van, T. T. 2018. "Development of the Statistical Model for Monitoring Salinization in the Mekong Delta of Vietnam Using Remote Sensing Data and In-Situ Measurements" *Proceedings* 2(10):565.

Wu, J., Vincent, B., Yang, J., Bouarfa, S., and Vidal, A. 2008. "Remote sensing monitoring of changes in soil salinity: a case study in Inner Mongolia, China" *Sensors* 8: 7035–7049.

Xiao, M., Zhang, G., Breitkopf, P., Villon, P., and Zhang, W. 2018. "Extended Co-Kriging interpolation method based on multi-fidelity data" *Applied Mathematics and Computation* 323: 120–131.

Zheng, Z., Zhang, F., Ma, F., Chai, X., Zhu, Z., Shi, J., and Zhang, S. 2009. "Spatiotemporal changes in soil salinity in a drip-irrigated field" *Geoderma* 149: 243–248.

ACKNOWLEDGMENT

This research was funded by the project VT-UD.03/16-20, under entitled: "Studying, Assessing, and Zoning Soil Salinity by Using Multi-temporal Satellite Imagery: A Case Study in Ben Tre Province", which belongs to the national program on Space Science and Technology (2016 – 2020).